

**Annealing effects on  $V_2O_{5-x}$  thin films deposited by non reactive sputtering**D. Rachel Malini<sup>1</sup>, R.Sivakumar<sup>2</sup>, C. Sanjeeviraja<sup>3,\*</sup><sup>1</sup>Department of Physics, The American College, Madurai-625002, India<sup>2</sup>Directorate of Distance Education, Alagappa University, Karaikudi-630004, India<sup>3</sup>Department of Physics, A.C. College of Engg. & Tech., Karaikudi-630004, India

sanjeeviraja@rediffmail.com

PACS 68

DOI 10.17586/2220-8054-2016-7-3-547-552

Thin films of vanadium oxide ( $V_2O_{5-x}$ ) were prepared by rf magnetron sputtering process and are heat treated to study the annealing effect. As-deposited thin films are amorphous in nature and crystallinity is improved by annealing the sample. Thin layers with high density and small grain size varying from 36 nm to 70 nm were seen in the FESEM images of as-deposited thin films. In the case of annealed thin films, it has been transformed to thin elongated rod like structure with 202.5 nm length and an average diameter of approximately 48 nm. Optical properties were studied by using UV-Vis-NIR spectrophotometer and the reduction in transmission in annealed thin films is due to the crystalline nature of thin films. Studies were done on the samples by taking photoluminescence and Laser Raman spectra.

**Keywords:** vanadium oxide, rf magnetron sputtering, annealing.*Received: 4 February 2016**Revised: 26 April 2016***1. Introduction**

Vanadium pentoxide ( $V_2O_5$ ), a transition metal oxide semiconductor, shows a wide range of applications in thin film form due to its multivalency, layered structure and wide optical band gap [1]. It is a promising compound for smart window applications, but the intercalation process is slow because of its low electrical conductivity and diffusion coefficient of ions [2–7]. Nanoparticle  $V_2O_5$  thin films are used to overcome this issue by increasing the surface area and decreasing the diffusion distance [8]. In our study, the experimental details for preparing sputtered  $V_2O_{5-x}$  thin films and the effect of annealing over the prepared thin films were discussed.

**2. Experimental**

$V_2O_{5-x}$  thin films were prepared on well cleaned Corning glass substrates (8 cm × 6 cm) by varying rf power as 150 W, 175 W and 200 W at room temperature. A target of 6 mm thickness and 50 mm diameter was obtained by pressing  $V_2O_5$  powder (99.9 % purity) in a pellatiser which was then sintered to 300 °C for about 2 hrs. The following parameters were kept constant during deposition of samples by non reactive sputtering process: 30 minutes deposition time,  $1.33 \times 10^{-2}$  mbar argon gas pressure and 6 cm target-substrate spacing. As-deposited thin films were then annealed at 400 °C for 5 hrs. Structural properties of thin films were studied by XRD using a XPERT-PRO PANalytical diffractometer with  $CuK\alpha$  radiation ( $\lambda=1.5406 \text{ \AA}$ ). The morphology of samples was studied using FEI's Quanta 200 FEG field emission scanning electron microscope (FESEM) and optical studies were undertaken by UV-vis-NIR spectrophotometer (HR-2000, M/s Ocean Optics, USA). PL spectra of samples were recorded at room temperature by using 'Varian Cary Eclipse Spectrophotometer' and Raman spectra were taken by Laser Raman spectrometer (Acton SpectraPro 2500i, Princeton Instruments, Acton Optics & Coatings).

**3. Results and Discussion**

XRD patterns of as-deposited and annealed  $V_2O_{5-x}$  thin films deposited on glass substrates by varying rf power from 150 W to 200 W are shown in Fig. 1. X-ray pattern of the  $V_2O_5$  target is also displayed for comparison. The target material exhibits 23 peaks corresponding to the orthorhombic  $V_2O_5$  phase at  $2\theta = 15.26^\circ, 20.15^\circ, 21.64^\circ, 25.48^\circ, 26.05^\circ, 30.92^\circ, 32.31^\circ, 33.28^\circ, 34.25^\circ, 41.2^\circ, 41.97^\circ, 45.38^\circ, 47.27^\circ, 47.75^\circ, 48.74^\circ, 51.16^\circ, 51.93^\circ, 55.57^\circ, 58.98^\circ, 61.02^\circ, 62.04^\circ, 68.71^\circ$  and  $74.39^\circ$  [JCPDS No: 89-2482]. It belongs to Pmmn space group having lattice parameters as  $a = 11.544 \text{ \AA}$ ,  $b = 3.571 \text{ \AA}$  and  $c = 4.383 \text{ \AA}$ . The maximum intensity with the height of 930.2 a.u. is displayed by the peak at  $2\theta = 20.15^\circ$  which proves that the  $V_2O_5$  target is oriented along (0 0 1) plane. The as-deposited  $V_2O_{5-x}$  thin films are gray in color [9]. XRD patterns of as-deposited thin films show very broad and diffuse patterns. There is no evidence for any diffraction peak and so these films are amorphous in nature. This shows that the plasma power of 200 W generated by the

rf was not enough for the growth of crystalline  $V_2O_{5-x}$  thin films in the absence of oxygen atmosphere during sputtering process [10]. With 0% oxygen content and  $V_2O_5$  as target during sputtering process, the deposited thin films are devoid of long range atomic order and are amorphous in nature. Generally, crystalline  $V_2O_5$  thin films are obtained by several authors by reactive sputtering under oxygen-argon mixture and also by choosing vanadium metal as target.

The annealed  $V_2O_{5-x}$  thin films deposited at low rf power are yellowish gray in color, whereas the samples prepared at high rf power are yellow in appearance, like  $V_2O_5$  powder [11]. The annealed thin film deposited at 175 W rf power shows peaks at  $2\theta = 17.71^\circ$  and  $28.64^\circ$  which are due to  $(\bar{2} 0 1)$  and  $(\bar{2} 0 2)$  plans of monoclinic  $VO_2$  phase [ JCPDS( 31-1438)]. In the annealed thin film prepared at 200 W rf power, two peaks were observed at  $2\theta = 12.58^\circ$  and  $17.71^\circ$  and are attributed to  $(1 0 1)$  plane of orthorhombic  $V_2O_5$  phase [JCPDS (85-2422)] and  $(\bar{2} 0 1)$  plane of monoclinic  $VO_2$  phase respectively. The crystallite size was calculated from the full width at half maximum (FWHM) of the  $V_2O_5$  phase in the annealed thin films deposited at 200 W rf power and is 60 nm. The crystallite size is 57 nm and 79 nm for the  $VO_2$  phase in the annealed thin films deposited at 175 W and 200 W respectively. This shows that the growth of  $VO_2$  phase in the annealed thin films improves with increase in rf power and this is due to the lack of oxygen during the sputtering process.

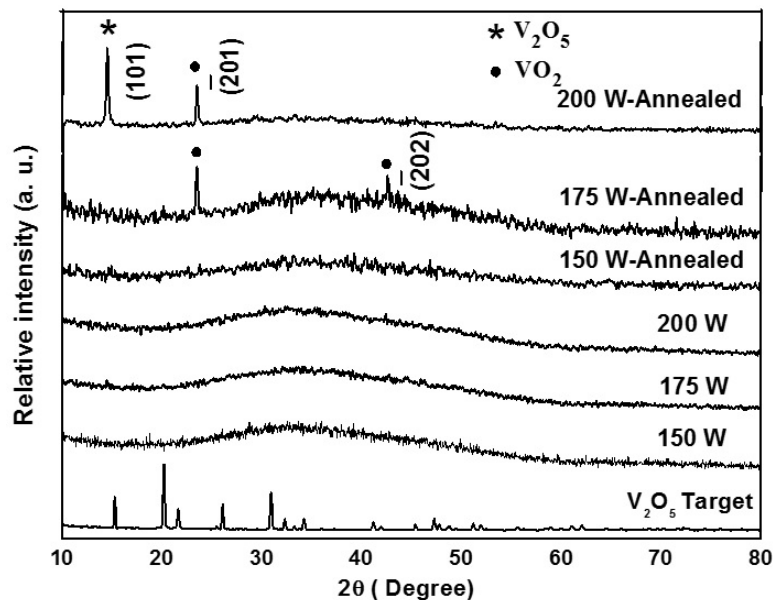


FIG. 1. XRD pattern of  $V_2O_5$  target, as-deposited and annealed  $V_2O_{5-x}$  thin films

Figure 2 shows the typical FESEM micrographs of as-deposited and annealed  $V_2O_{5-x}$  thin films deposited at 200 W rf power. Thin layers with high density and small grain size varying from 36 nm to 70 nm are seen in FESEM images of as-deposited thin films. Unlike the as-deposited thin films, annealed  $V_2O_{5-x}$  thin films deposited at 175 W rf power contain individual and separate grains (not shown). The grain size of such annealed thin films increases with increase in rf power and the grain shape varies from small granular surface structure to elongated thin rectangular bars when rf power increases from 175 W to 200 W. The granular spherical shape grains show an average diameter of 324 nm in annealed thin films deposited at 175 W rf power. Annealed thin films deposited at 200 W rf power show thin elongated rod like structure with approximately 202 nm length and average diameter of 48 nm. Because of the formation of new bonds which results in densification, grain growth is encouraged in annealed thin films [12].

Figure 3(a) shows the transmission of as deposited and annealed thin films deposited by varying rf power over the wavelength range of 300 – 900 nm.  $V_2O_{5-x}$  thin films deposited at 150, 175 and 200 W rf power have transmittance values of 80 %, 84.1 % and 92.9 % respectively. The high transmission indicates that thin films deposited at 200 W rf power are weakly absorbing in the spectral range of 450 to 1000 nm and the decrease in transmission at  $\lambda < 400$  nm is due to the fundamental absorption. These data are consistent with previous reports [13]. The transmittance values for the annealed samples are recorded as 61 %, 43.9 % and 30.7 %. The surface of annealed samples becomes rough, resulting in light loss by scattering and thus low transmittance [14,15]. In annealed thin films the absorption peak at around 350 nm was red-shifted with an increase in rf power [16].

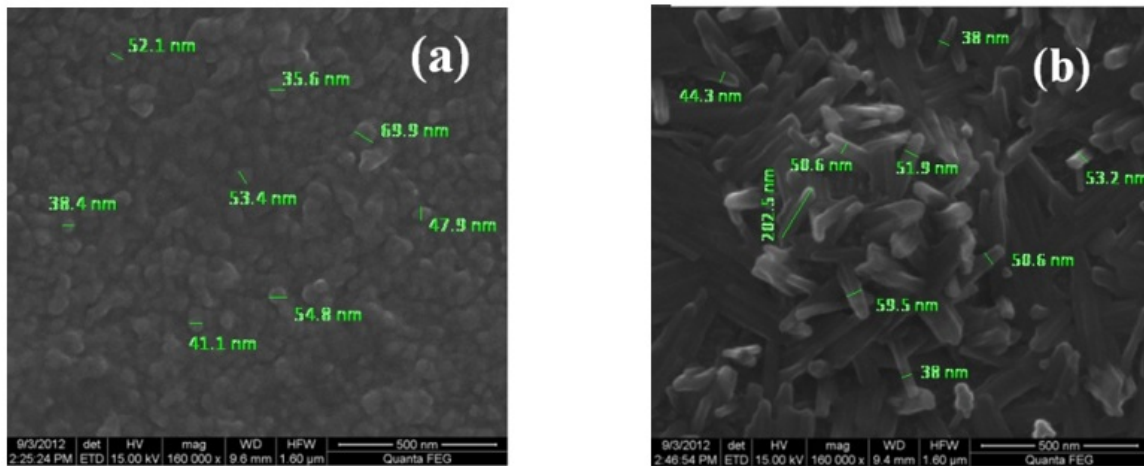


FIG. 2. FESEM images of (a) as-deposited and (b) annealed thin films at 200 W rf power

The experimental data were found to give a better fit when  $(\alpha h\nu)^{1/2}$  was plotted against  $h\nu$ . This suggests an indirect allowed transition. Fig. 3(b) shows the relation between  $(\alpha h\nu)^{1/2}$  and photon energy for as-deposited and annealed thin films prepared by varying rf power.  $E_g$  of as-deposited thin films increases as 2.10, 2.35 and 2.45 eV with increase in rf power. High rf power during deposition favors the formation of  $V_2O_5$  phase in thin films by partially filling oxygen vacancies, thereby reducing localized states and hence the bandgap increases. The optical bandgap of annealed thin films decreases as 1.40, 1.26 and 1.18 eV with increase in rf power. Excess electrons are localized at the empty 3-d orbital of vanadium atoms which are closer to oxygen vacancy and thus localized states are developed in the bandgap and hence a decrease in bandgap energy [17].

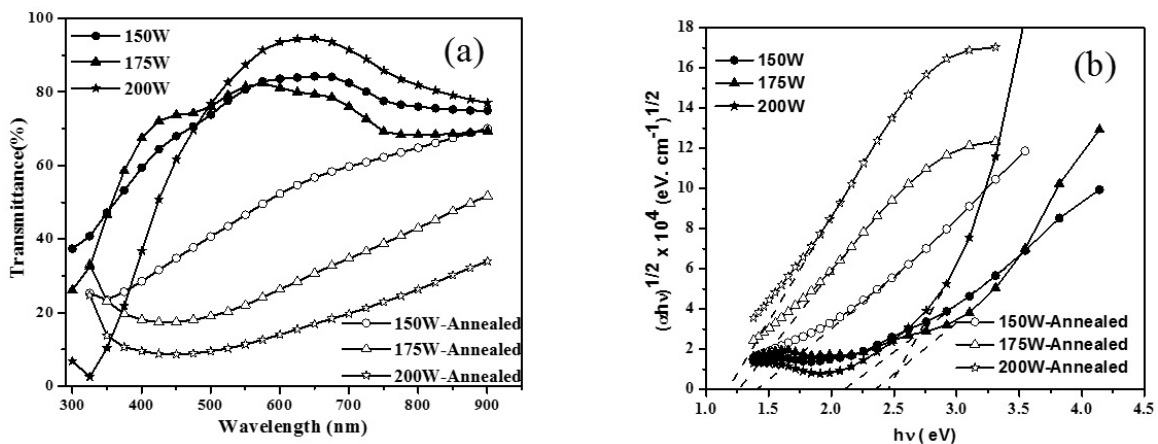

 FIG. 3. (a) Transmittance spectra and (b) Optical bandgap of  $V_2O_{5-x}$  thin films

Figure 4(a) shows the PL spectra of  $V_2O_{5-x}$  thin films deposited at various rf power recorded at room temperature by using the instrument 'Varian Cary Eclipse Spectrophotometer' where the source is the Xe lamp. PL emission peaks of as-deposited thin films exhibit a blue shift when rf power increases. The presence of emission wavelength at around 600 nm for the excitation wavelength of 460 nm indicates the existence of defects on the surface of thin films as oxygen vacancies [18]. The optical bandgap energy values have been calculated from the emission wavelength and are obtained as 1.93, 2.05 and 2.3 eV with respect to 150, 175 and 200 W rf power. The calculated bandgap energy values are in good agreement with those obtained from UV-Vis-NIR spectrophotometer studies. The PL spectra of annealed thin films deposited at various rf power for the excitation wavelength of 460 nm were recorded at room temperature and are shown in Fig. 4(b). The PL emission peaks of annealed thin films exhibit a red shift by positioning at 749, 759 and 774 nm for 150, 175 and 200 W rf power respectively. From the emission wavelength, the energy bandgap values for thin films of 150, 175 and 200 W rf power during deposition have been calculated as 1.66, 1.64 and 1.60 eV respectively. The emission peak at around 759 nm

indicates that the samples could emit intensely visible light at room temperature and is due to defects such as oxygen vacancies which got involved during growth [19]. This result is confirmed by Yu-quan Wang [20] by fitting two Gaussian peaks in the PL spectrum centered at approximately 650 and 730 nm, which correspond to energies of approximately 1.82 and 1.68 eV, respectively. Since the band gap of  $V_2O_5$  is approximately 2.24 eV, they deduced that these visible emissions are caused by oxygen defects.

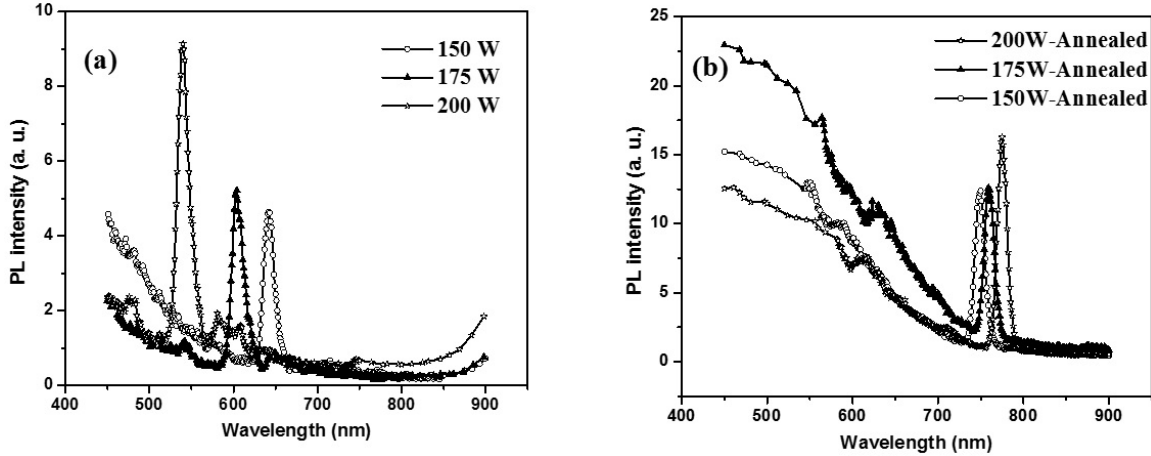


FIG. 4. (a) PL emission spectra of  $V_2O_{5-x}$  thin films deposited at various rf power and (b) their respective annealed samples

Figure 5(a) shows the Raman spectra of  $V_2O_{5-x}$  thin films deposited at different rf power along with that of  $V_2O_5$  target material. The target material exhibits two sharp peaks at  $785.99\text{ cm}^{-1}$  and  $902.10\text{ cm}^{-1}$  which are due to the V–O–V stretching vibration mode [21] and the  $V^{4+} = O$  bond which is created by the modification in  $V^{5+} = O$  vanadyl oxygen stretching mode [22] respectively. The corner shared oxygens in common to the two pyramids exhibit another stretching mode as  $V_2-O$  and the peak corresponding to it is located at  $702.84\text{ cm}^{-1}$  in the target material [23]. Two flat and small peaks are visible at  $1004.63\text{ cm}^{-1}$  and  $1071.81\text{ cm}^{-1}$  and a broad peak at  $1175.34\text{ cm}^{-1}$  which corresponds to the terminal oxygen (V=O) stretching modes due to the unshared oxygen [24]. Raman spectra of as-deposited thin film prepared at 150 W rf power exhibits a peak at  $1053.57\text{ cm}^{-1}$  which corresponds to the terminal oxygen (V=O) stretching mode due to the unshared oxygen. A flat peak is also observed at  $943.12\text{ cm}^{-1}$  which is due to the  $V^{5+} = O$  vanadyl oxygen stretching mode modification. Five peaks are observed in the Raman spectrum of thin film deposited at 175 W rf power and are located at  $706.23$ ,  $839.46$ ,  $938.59$ ,  $986.39$  and  $1051.30\text{ cm}^{-1}$ . The new peak at  $705.87\text{ cm}^{-1}$  in the Raman spectrum is due to the stretching vibration of  $V_2 - O$  bond [25]. The flat peak due to the modification in  $V^{5+} = O$  vanadyl oxygen stretching mode to  $V^{4+} = O$  appears as a sharp one with intensity of 107.96 a.u. at  $938.59\text{ cm}^{-1}$ . The terminal oxygen stretching mode due to the unshared oxygen is responsible for the new Raman peak at  $986.39\text{ cm}^{-1}$ . The emergence of the Raman inactive mode at  $839.46\text{ cm}^{-1}$  again confirms the amorphous nature of the prepared thin film. The red shift of the peak due to the terminal oxygen (V=O) stretching mode from  $1053.57\text{ cm}^{-1}$  to  $1051.30\text{ cm}^{-1}$  with increase in intensity from 56.39 to 66.59 a.u. also confirms the structural disorder resulting in the amorphous nature of the thin films prepared. Six Raman peaks with low intensities are observed in the Raman spectrum of thin film deposited at 200 W rf power and are located at  $773.41$ ,  $863.36$ ,  $900.97$ ,  $944.25$ ,  $993.18$  and  $1151.44\text{ cm}^{-1}$ . The first peak at  $773.41\text{ cm}^{-1}$  is due to the V-O-V stretching vibration mode and the peaks at  $900.97$  and  $944.25\text{ cm}^{-1}$  correspond to the  $V^{4+} = O$  bond which is created by the modification in  $V^{5+} = O$  vanadyl oxygen stretching mode. This modification is due to basic point defects in the  $V_2O_{5-x}$  crystal lattice i.e. the oxygen vacancies created by removing vanadyl oxygen and thereby generating reduced  $V^{4+}$  from  $V^{5+}$  ions. The seventh peak of the Raman spectrum corresponds to the terminal oxygen (V=O) stretching mode due to the unshared oxygen and is located at  $1049.04\text{ cm}^{-1}$  with high intensity of 80.86 a.u.

Figure 5(b) shows Raman spectra of annealed thin films deposited at different rf powers. Apart from the two sharp peaks at  $1007.98$  and  $1129.8\text{ cm}^{-1}$  due to  $V^{5+} = O$  bond of terminal oxygen atoms, the Raman spectrum of annealed  $V_2O_{5-x}$  thin films deposited at 150 W rf power shows two low intensity peaks at  $766.49$  and  $846.25\text{ cm}^{-1}$ . The peak observed at  $846.25\text{ cm}^{-1}$  corresponds to infrared active mode and is Raman inactive for a well-crystalline  $V_2O_5$  material. When a non-stoichiometric  $V_2O_5$  thin film with structural disorders is analyzed, this mode becomes active [26]. The Raman spectrum of annealed thin films deposited at 175 W rf power shows

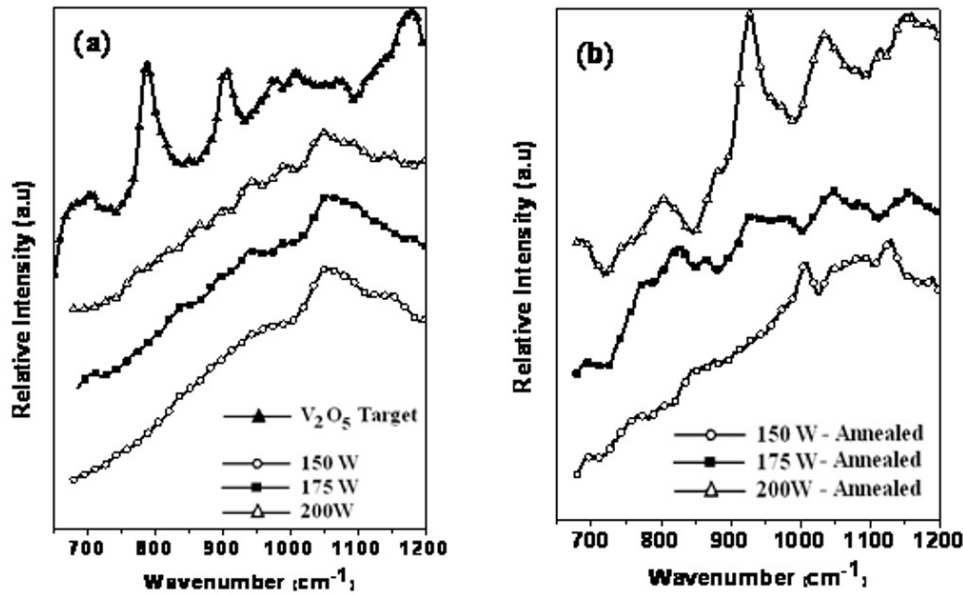


FIG. 5. (a) Raman spectra of  $V_2O_{5-x}$  thin films deposited at various rf power and (b) their respective annealed samples

four peaks at 824.11, 930.535, 1049.04 and 1158.36  $\text{cm}^{-1}$ . The peaks corresponding to the stretching mode due to  $V^{5+} = O$  bond of terminal oxygen atoms are shifted to high energy region at 1049.04 and 1158.36  $\text{cm}^{-1}$  with increase in intensities and this shows that the annealed thin films are heading towards  $V_2O_{5-x}$  phase. Along with that, a peak due to  $V^{4+} = O$  bond is also seen at 939.9  $\text{cm}^{-1}$  which proves the presence of  $VO_2$  in annealed thin films. The peak corresponding to the Raman inactive mode appears at 824.11  $\text{cm}^{-1}$ . The absence of external low frequency modes at 104, 142 and 194  $\text{cm}^{-1}$  indicates that the prepared thin films are lagging in layered  $V_2O_{5-x}$  crystalline structure. The Raman spectrum of annealed thin films deposited at 200 W rf power exhibits well resolved Raman lines which indicate the crystallinity of thin films. The high intensity Raman peak at about 928.15  $\text{cm}^{-1}$  is related to the vanadyl stretching mode corresponding to  $V=O$  bond in the crystal structure and this is attributed to the  $V^{4+} = O$  bonds. These  $V^{4+} = O$  bonds arise due to the direct conversion from  $V^{5+} = O$  bonds or the breaking of the single oxygen bonds which involves  $V^{4+}$  ions or both. The shift of this peak towards low frequency range indicates the presence of structural disorder in the annealed thin films at high rf power and this is confirmed by the presence of the peak at 804.23  $\text{cm}^{-1}$  which corresponds to the IR active mode. The two broad peaks at 1032.95 and 1151.32  $\text{cm}^{-1}$  are assigned to the stretching mode due to  $V^{5+} = O$  bond of terminal oxygen atoms on the surface clusters of annealed thin films. The generation of a new peak at 684.59  $\text{cm}^{-1}$  is due to the stretching vibration mode of  $V_2 - O$  bond in the  $V-O-V$  disordered framework. If sufficient oxygen pressure was allowed during deposition, this peak would have exhibited a red shift and would be 706  $\text{cm}^{-1}$  which is the stretching mode of the crystalline  $V_2O_{5-x}$  thin films arising due to the corner sharing oxygen atoms of two successive pyramids.

#### 4. Conclusion

In this paper, annealing effects on  $V_2O_{5-x}$  thin films deposited by varying rf power have been studied. As-deposited thin films are amorphous in nature and their crystallinity is improved by annealing. Nanoscale grains are seen in as-deposited thin films and were then transformed into rectangular rods after annealing. The optical bandgap for annealed thin films decreases with increase in rf power and is due to development of localized states. PL spectra of as-deposited thin films show blue shift in emission peak at 600 nm with increase in rf power and annealed samples exhibit a reverse effect. Apart from the peak due to  $V=O$  stretching mode, a Raman peak is observed at 928.1  $\text{cm}^{-1}$  in annealed thin films deposited at 200 W rf power and is attributed to  $V^{4+} = O$  bonds.

## References

- [1] Rajendra Kumar R.T., Karunakaran B., et al. Structural properties of  $V_2O_5$  thin films prepared by vacuum evaporation, *Mat. Sci. Semicon. Proc.*, 2003, **6**, P. 543–546.
- [2] Takahashi K., Wang Y., Cao G. Growth and electrochromic properties of single-crystal  $V_2O_5$  nanorod arrays. *Appl. Phys. Lett.*, 2005, **86**, P. 053102-1–053102-3.
- [3] Ramana C.V., Hussain O.M., et al. Physical investigations on electron-beam evaporated vanadium pentoxide films. *Mater. Sci. Eng. B*, 1998, **52**, P. 32–39.
- [4] Fujita Y., Miyazaki K., Tatsuyama C. On the electrochromism of evaporated  $V_2O_5$  films. *Jpn. J. Appl. Phys.*, 1985, **24**, P. 1082–1086.
- [5] Kim B.H., Kim A., et al. Energy gap modulation in  $V_2O_5$  nanowires by gas adsorption. *Appl. Phys. Lett.*, 2008, **93**, P. 233101–233103.
- [6] Raible I., Burghard M., et al.  $V_2O_5$  nanofibres: novel gas sensors with extremely high sensitivity and selectivity to amines. *Actuat. B*, 2005, **106** P. 730–735.
- [7] Moshfegh A.Z., Ignatiev A. Formation and characterization of thin film vanadium oxides: Auger electron spectroscopy, X-ray photoelectron spectroscopy, X-ray diffraction, scanning electron microscopy, and optical reflectance studies. *Thin Solid Films*, 1991, **198** P. 251–268.
- [8] Wang Y., Takahashi K., Shang H., Cao G. Synthesis and Electrochemical Properties of Vanadium Pentoxide Nanotube Arrays. *J. Phys. Chem. B*, 2005, **109**, P. 3085–3088.
- [9] Alaa A. Akl. Crystallization and electrical properties of  $V_2O_5$  thin films prepared by RF sputtering. *Appl. Surf. Sci.*, 2007, **25**, P. 7094–7099.
- [10] Rachel Malini D., Sanjeeviraja C. Effect of RF power on electrochromic V-Ce mixed oxide thin films. *Electrochim. Acta*, 2013, **104**, P. 162–169.
- [11] Wu G., Du K., et al. Optical absorption edge evolution of vanadium pentoxide films during lithium intercalation. *Thin Solid Films*, 2005, **485**, P. 284–289.
- [12] Kingery W.D. in: W. Kingery (Ed). *Kinetics of High Temperature Process*. MIT Press, Cambridge, MA., 1959, P. 187.
- [13] Michailovits L., Hevesi Liem phan I., Varga Zs. Determination of the optical constants and thickness of amorphous  $V_2O_5$  thin films. *Thin Solid Films*, 1983, **102**, P. 71–76.
- [14] Meng L.-J., Silva R.A., et al. Optical and structural properties of vanadium pentoxide films prepared by d.c. reactive magnetron sputtering. *Thin Solid Films*, 2006, **515**, P. 195–200.
- [15] Cui H.-N., Teixeira V., et al. Thermo-chromic properties of vanadium oxide films prepared by dc reactive magnetron sputtering. *Thin Solid Films*, 2008, **516**, P. 1484–1488.
- [16] Guan Z.S., Yao J.N., Yang Y.A., Loo B.H. Electrochromism of annealed vacuum-evaporated  $V_2O_5$  films. *J. Electroanal. Chem.*, 1998, **443**, P. 175–179.
- [17] Ramana C.V., Hussain O.M., Srinivasulu Naidu B., Reddy P.J. Spectroscopic characterization of electron-beam evaporated  $V_2O_5$  thin films. *Thin Solid Films*, 1997, **305**, P. 219–226.
- [18] Wu M.-C., Lee C.-S. Field emission of vertically aligned  $V_2O_5$  nanowires on an ITO surface prepared with gaseous transport. *J. Solid State Chem.*, 2009, **182**, P. 2285–2289.
- [19] Wang Y.Q., Li Z.C., et al. Synthesis and optical properties of  $V_2O_5$  nanorods. *J. Chem. Phys.*, 2007, **126**, P. 164701(1)–164701(3).
- [20] Wang Y.Q., Li Z.C., Zhang Z.J. Preparation of  $V_2O_5$  thin film and its optical characteristics. *Front. Mater. Sci. China*, 2009, **3**, P. 44–47.
- [21] Subba Reddy Ch.V., Park K.-Il, et al. Simple preparation of  $V_2O_5$  nanostructures and their characterization. *Bull. Korean Chem. Soc.*, 2008, **29**, P. 2061–2064.
- [22] Lee S.H., Cheong H.M., et al. Raman spectroscopic studies of amorphous vanadium oxide thin films. *Solid State Ionics.*, 2003, **165**, P. 111–116.
- [23] Chen W., Mai L., et al. Raman spectroscopic study of vanadium oxide nanotubes. *J. Solid State Chem.*, 2004, **177**, P. 377–379.
- [24] Lee S.H., Cheong H.M., et al. Improving the Durability of Amorphous Vanadium Oxide Thin-Film Electrode in a Liquid Electrolyte. *Electrochem. Solid-State Lett.*, 2003, **6**, P. A102–A105.
- [25] Julien C., Nazri G.A., Bergstrom O. Raman Scattering Studies of Microcrystalline  $V_6O_{13}$ . *Phys. Status solidi.B.*, 1997, **201**, P. 319–326.
- [26] Julien C., Guesdon J.P., et al. The influence of the substrate material on the growth of  $V_2O_5$  flash-evaporated films. *Appl. Surf. Sci.*, 1995, **90**, P. 389–391.